Scandinavian Journal of Forest Research

ISSN: 0282-7581 (Print) 1651-1891 (Online) Journal homepage: http://www.tandfonline.com/loi/sfor20

Small area estimations of proportion of forest and timber volume combining Lidar data and stereo aerial images with terrestrial data

Katharina Steinmann , Daniel Mandallaz , Christian Ginzler & Adrian Lanz

To cite this article: Katharina Steinmann , Daniel Mandallaz , Christian Ginzler & Adrian Lanz (2013) Small area estimations of proportion of forest and timber volume combining Lidar data and stereo aerial images with terrestrial data, Scandinavian Journal of Forest Research, 28:4, 373-385, DOI: 10.1080/02827581.2012.754936

To link to this article: https://doi.org/10.1080/02827581.2012.754936

Accepted author version posted online: 05 Dec 2012.
Published online: 10 Jan 2013.

Scandinavian Journal of Forest Research, 2013
Vol. 28, No. 4, 373–385, http://dx.doi.org/10.1080/02827581.2012.754936

Taylor & Francis
Taylor & Francis Group

RESEARCH ARTICLE

Small area estimations of proportion of forest and timber volume combining Lidar data and stereo aerial images with terrestrial data

KATHARINA STEINMANN[1], DANIEL MANDALLAZ[2], CHRISTIAN GINZLER[3] & ADRIAN LANZ[1]

[1]*Forest Resources and Forest Management Unit, Swiss Federal Research Institute WSL, Birmensdorf, Switzerland,* [2]*Institute for Terrestric Ecosystems, Swiss Federal Institute of Technology Zürich ETH, Zürich, Switzerland, and* [3]*Land Use Dynamics Unit, Swiss Federal Research Institute WSL, Birmensdorf, Switzerland*

Abstract
Methods for small area estimations were compared for estimating the proportion of forest and growing stock volume of temperate mixed forests within a district of a member state (canton) in Switzerland. The estimators combine terrestrial data with remotely sensed auxiliary data. By using different model types, different sources of auxiliary data and different methods of processing the auxiliary data, the increase in estimation precision was tested. Using the canopy height derived from remote sensing data, the growing stock volume and the proportion of forest were estimated. The regression models used for the small area estimation provided a coefficient of determination of up to 68% for the timber volume. The proportion of plots correctly classified into forest and non-forest plots ranged between 0.9 and 0.98. Models calibrated over forest area only resulted in a maximal coefficient of determination of 37%. Even though these coefficients indicate a moderate model quality, the use of remote sensing data clearly improved the estimation precision of both the proportion of forest and the growing stock volume. Generally, Lidar data led to slightly higher estimates compared to data from aerial photography. It was possible to reduce the variance of the estimated proportion of forest to nearly one tenth compared with the variance based on the terrestrial measurements alone. Similarly, the variance of the growing stock volume could be reduced to one fourth as compared with the variance based solely on the terrestrial measurements.

Keywords: *Canopy height, regression estimator, small-area estimation, growing stock volume.*

Introduction

Information from national forest inventories is used in many fields such as forest management and political decision making on both national and regional levels (McRoberts et al. 2010b). However, national forest inventories are expensive and time consuming. The sampling density is therefore limited and the acquisition of reliable information over small scales difficult. Today, forest information at a local scale is therefore commonly obtained by combining field data with remote sensing data using multispectral satellite imagery (Reese et al. 2002; McRoberts et al. 2007) or aerial photographs (Uuttera et al. 1998; Holmström et al. 2001; St-Onge et al. 2008; Bohlin et al. 2012). Remote sensing data can be used to model a wide set of selected variables. On the tree level, these include tree height (Næsset 1997; Magnussen et al. 1999), basal area (Franklin 1986; Wolter et al. 2008) and crown size (Wu & Strahler 1994; Song et al. 2010). On the forest stand level, estimates can be made of crown canopy, species composition (Waser et al. 2010, 2011) and stem density (Hudak et al. 2006; McRoberts et al. 2006), as well as stand age (Maltamo et al. 2009). Remote sensing data thus have great potential to either reduce inventory costs or increase the precision of estimates made within a given budget (Eid et al. 2004; Næsset et al. 2004; McRoberts et al. 2006). Auxiliary data from aerial images, laser, or satellite data can also be used to estimate population parameters in small areas for which terrestrial data are scarce (Tomppo et al. 2008, Næsset et al. 2011; Breidenbach & Astrup 2012).

Correspondence: Katharina Steinmann, Forest Resources and Forest Management Unit, Swiss Federal Research Institute WSL, Zürcherstr. 111, CH-8903 Birmensdorf, Switzerland. E-mail: Katharina.Steinmann@wsl.ch

(*Received 20 February 2012; accepted 26 November 2012*)

In the context of forest inventory, the concept of small area estimation refers primarily to the problem of getting estimates for a geographical area G, which is a subset of the entire forested area F within a region or the entire country for which the inventory was designed. "Small" is of course a relative concept. It does not necessarily imply that the number of plots (with remote sensing data in the first phase and terrestrial data on a subset in the second phase) is small, though this is often the case for the second phase. The key issue is that the models used to obtain terrestrial predictions at all plots where remote sensing data are available are fitted from the global inventory data. The mean of the residuals is zero over F (or very close to zero) for internal models, i.e. fitted by least squares like techniques with the inventory data at hand, whereas it is generally different from zero over G.

If the number of terrestrial plots in G is very small, even zero, one often relies on the synthetic estimator (Särndal et al. 1992), which is simply the mean of the predictions. (Usually, a sufficiently large number of first-phase plots are available in G, see, e.g. Rao [2003].) Theoretically, a synthetic estimator can be analysed from a purely model-dependent point of view or within the design-based approach (Gregoire 1998, 2011). Model-assisted estimators can be considered as an intermediate approach between the model-dependent and the design-based approach. They rely on observations for population units selected for the sample and model predictions for population units not selected for the sample. However, because the validity of an inference is still based on the probability sample, the estimator is characterised as probability based (Stehman 2009). The basic statistical difference between probability- and model-based inferences relies on the source of randomization. With the probability-based inference, randomization enters into the sample through the random selection of the population units, whereas randomization for model-based inference enters through the random realizations from the distributions of response variables for population units (McRoberts et al. 2010a).

The drawback of the synthetic estimator is that it can have a large design-based bias. If the number of residuals (second-phase plots) in G is sufficiently large, one can correct the design bias of the synthetic estimator by adding the mean residual over G to obtain the small-area estimator. The inference and, in particular, the calculation of the variances, also for the synthetic estimator, are design based.

In this paper, we follow the model-assisted approach: we use models to increase the accuracy of estimators but the variance is calculated under the sampling design, assuming that one can treat systematic samples (grids) as simple random samples. This is legitimate for extensive inventories as the variance is usually slightly overestimated (see Mandallaz [2008], Chapters 7 and 8). As long as the small area has similar properties to the large area, estimates obtained with the synthetic estimator will be close to estimates obtained with the simple random sample estimator (hereafter called the direct estimator) and to the residual corrected small area estimator. If the properties differ, the synthetic estimator can under- or overestimate the real (unknown) target parameter. The synthetic estimator can thus be severely design biased. When the small area is large enough to contain some sampling elements, the synthetic estimation can be corrected with the residuals to obtain the difference estimator or small area estimator, which is approximately design unbiased (Särndal et al. 1992; Rao 2003; Mandallaz 2008; Lanz et al. 2009). From the economic point of view, the forest area, the growing stock volume and the resultant wood biomass are especially important. As both the differentiation between forest- and non-forest areas and the growing stock within the forest area are well correlated with the canopy height, a digital surface model is often used as auxiliary information. Information about the canopy height can be taken from light detection and ranging (Lidar) technology or from photogrammetric processing using aerial images (Kovats 1997; Katsch & Stocker 2000; Hildebrandt 2010; Latifi et al. 2010).

In the present study, we derived auxiliary data from aerial images as well as from Lidar data and combined it with terrestrial data from the Swiss National Forest Inventory. The aim was to test and compare different methods of small area estimations for the forest area and the growing stock volume of temperate mixed forests. Specifically, we tested and compared different methods to derive auxiliary information as well as different statistical models and different sizes of sampling grids.

Materials and Methods

Study Area

As a test area, we used the northwest part of Switzerland, which covers the area of the Swiss central Plateau and the Jura (see Figure 1). With an area of 14,325 km^2, the two production regions cover roughly one third of the total Swiss state area. The canton of Aargau with an area of roughly 1400 km^2 was used as small area, where we derived the auxiliary data within quadrats with a side length of 25 m, which were arranged on a grid of 500×500 m (detailed information about the sampling sizes is

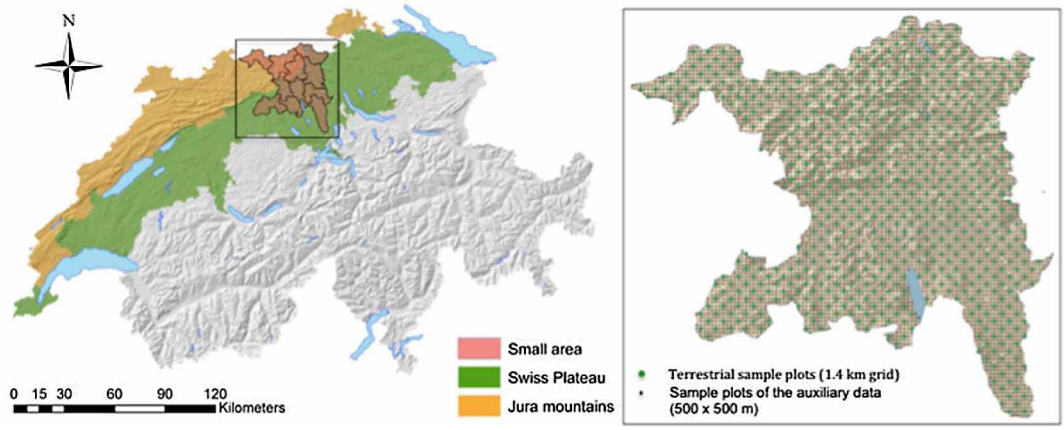

Figure 1. Maps of the study area and sample plots within the small area.

given in Table I). Within the canton of Aargau, the proportion of the area covered by the Jura region to the area covered by the Swiss Plateau is about 1:2, which is approximately the same as in the total area used for the model calibration.

Terrestrial Data

In Switzerland, the National Forest Inventory (SNFI) has been monitoring the state and dynamics of Swiss forests since 1982. Every 10 years, forest variables are measured in the field. For the present study, the response variables were assessed from field surveys of the third NFI, measured between 2004 and 2006 (Brändli 2010). The sampling plots of the third NFI are aligned in a grid with a mesh size of 1.4 km. Taking the diagonal of a 1.4- $\times$1.4-km quadrat as a side length to build a second grid with half the number of sampling plots of the first grid produced a new grid with a mesh size of 2 km. Repeating this procedure led to less dense grids with mesh sizes of 2.8 and 4 km.

A sampling plot is classified as such when its centre belongs to a woodland area. The forest/non-forest decision is defined as a binomial quantity (1 = forest, 0 = non-forest). Only trees belonging to a forest plot were measured. Two concentric circles, with an area of 200 and 500 m^2, respectively, represent a sampling plot. Within the smaller circle of a sampling plot, trees with a diameter at breast height (DBH) $\geq$12 cm are recorded. Within the larger circle, trees with a DBH $\geq$36 cm are recorded. Individual tree volumes were estimated with allometric models and served as the basis for the standing timber estimation. As estimations of the bole volume based only on the diameter at breast height are less precise than estimations that are additionally based on the tree height and an upper stem diameter (diameter at 7-m height), so-called tariff trees were measured on a subsample (Kaufmann 1999). Volume estimations of the tariff trees were used to derive tariff models. These models estimated individual tree volumes by one measurement only (the diameter at breast height) but additionally include tree, stand and site attributes such as tree species, production regions, storey to which a tree belongs and bifurcation of a stem (for details see Kaufmann 1999). Per definition, the growing stock volume of non-forest plots was set to zero. The growing stock volume of the forest sampling area is the represented (local) hectare density (m^3/ha).

Table I. Sample sizes of the different grids in the test area.

	Number of samples			
Sampling grids	Total	Thereof forest plots	Within the small area	Thereof forest plots
Ancillary data (n_1)				
500 m $\times$500 m grid	10,622	3560	5530	1987
Terrestrial data (n_2)				
1.4 km $\times$1.4 km sampling grid	5697	1777	682	222
2 km $\times$2 km sampling grid	5358	1662	343	107
2.8 km $\times$2.8 km sampling grid	5183	1622	168	67
4 km $\times$4 km sampling grid	5100	1591	85	36

Auxiliary Data

We tested models using the canopy height to predict the growing stock volume. In addition, a measurement for the patchiness of the forest, defined as the number of clusters of contiguous forest pixels within a square sample unit of 25 × 25 m with the terrestrial plots as centres, was tested as a potential auxiliary variable.

The auxiliary data were basically derived from stereo-aerial images and airborne laser scanner data. The stereo-aerial images were taken between 2006 and 2008 from an airborne digital sensor (Leica ADS40). The line-scan sensor acquires simultaneously nadir, backward and forward images. Using the off-the-shelf SocetSet software (5.4.1, BAE) for image correlation, a digital surface model with a resolution of 1 m was calculated.

The digital terrain model (DTM) was interpolated from the last pulse Lidar data. The average point density was 0.85 points/m^2. According to Swisstopo, the precision of the height (1 SD) is ±0.5 m. The canopy height model (CHM) was estimated from the difference between the digital surface model and the DTM. The distance of the derived elevation (z-value) of the first pulse Lidar data to the DTM was used as alternative information for the canopy height.

The mean canopy heights within squared areas with side lengths of 25 m centred on the terrestrial sampling plots were used to predict the growing stock volume. In the case of the aerial photography data, the canopy height was estimated by the mean of 625 (25 × 25) pixel values from the CHM. In the case of the Lidar data, the canopy height was estimated by the mean of all canopy height values from the first pulse data, which dropped into a 25- × 25-m quadrat centred on the sampling plots. As the precision of estimates not only depends on the model type but also on the data quality, additional approaches were tested to derive information about the canopy height. Specifically, we tested the mean of the canopy height values, which exceeded the median within the corresponding quadrats around the terrestrial sampling plots. Similarly, we calculated the mean canopy heights where only pixel values above the 75th, 90th and 95th percentiles, respectively, were considered (see Figure 2 for the different ways of processing the remote sensing data). The same pixel selection was applied to calculate the variance of the canopy heights within the quadrats around the sampling plots. In cases where the canopy height of a sampling plot was negative, it was set to zero. If the canopy height was higher than 50 m, it was set to 50 m, as we assumed that canopy heights above 50 m are not realistic. By constraining the predictive variables, unrealistic predictions are avoided. Furthermore, restricting the predictive variables to the number range between 0 and 50 guarantees that the range of the predictors of the population does not exceed the range of the predictors of the sample, and hence a potential distortion of extrapolations by applied models is excluded.

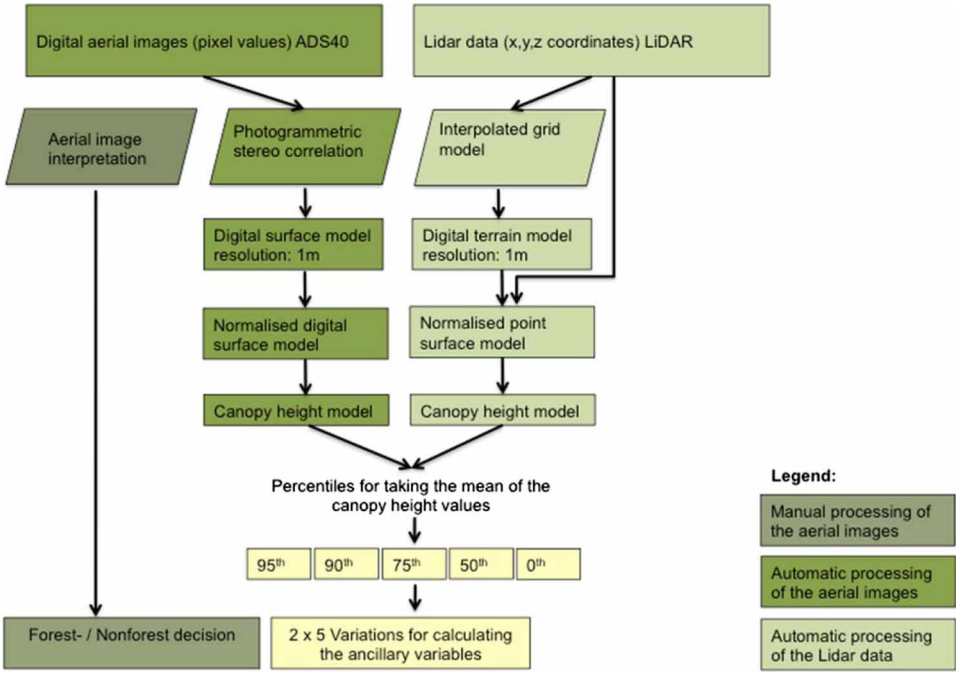

Figure 2. Data processing of the remote sensing data.

In order to test a potential forest boundary effect on the growing stock volume, we generated measures, which took the patchiness of the forest into account. We therefore generated a tree mask, which was based on the CHM. Pixels with a canopy height value exceeding a threshold value of 5 m were classified as forest (with a value of 1), whereas the rest of the pixels were classified as non-forest (with a value of 0). Based on the queen's structure (i.e. 8 neighbouring cells), the number of clusters of connected forest cells of the tree mask was calculated and the patchiness of the forest around the terrestrial sampling plots was thus quantified. A measure for the forest boundary was calculated in two steps. First, for each grid cell, the number of forest cells within the 3×3 neighbouring pixel area was counted and stored in a new grid layer. Then, the mean of all pixel values (which ranged from 0 to 8) of the new grid layer was calculated within the same 25- $\times$25-m quadrats used above. This index was used to quantify forest boundaries within a given area.

For some models, we used the forest/non-forest decision from the aerial photograph interpretation of the SNFI as a further predictor. A forest/non-forest decision was made by the aerial photograph interpreters for each sampling plot of the 500- $\times$500-m grid, independent of the forest/non-forest decision from the terrestrial inventory. For further details, see Ginzler et al. (2005) or Mathys et al. (2006).

In a further approach, the forest/non-forest decision for the plots of the 500- $\times$500-m grid was predicted from the CHM. Based on the canopy height, the probability of the presence of forest was predicted with logistic regression models (McCullagh & Nelder 1999), where the terrestrial forest/non-forest decisions served for the model calibration. Sampling plots for which a probability of the presence of forest was higher than 50% were defined as forest plots. The rest of the sampling plots were considered as non-forest plots (McRoberts 2006, 2010).

In summary, 22 predictors were tested for their suitability in predicting timber volumes: Five different measurements of canopy height, derived from five different percentiles used for averaging the mean canopy height, were tested for the aerial photography and the Lidar data, resulting in 10 potential predictors. The corresponding variations were tested as predictors, which potentially carry information about the forest structure, thus leading to another 10 potential predictors. Measurements for patchiness and forest boundary layer were derived from the ADS40 data. The canopy heights derived from the different percentiles and different sources of remote sensing data were also tested for the prediction of the forest/non-forest decision. In addition, the forest/non-forest decision from the aerial photograph interpretation was used to model the terrestrial forest/non-forest decision.

Statistics

The direct, one-phase estimator was used as reference for the estimation of the mean spatial density of the target variable in the small area:

$$\hat{Y}_{dir,k} = \frac{1}{n_{2,k}} \sum_{x \in s_{2,k}} Y(x) \tag{1}$$

Its estimated design-based variance is given by

$$\hat{V}(\hat{Y}_{dir,k}) = \frac{1}{n_{2,k}} \hat{V}(Y(x)_k), \tag{2}$$

where

$$\hat{V}(Y(x)_k) = \frac{1}{n_{2,k} - 1} \sum_{x \in s_{2,k}} (Y(x) - \overline{Y}_{2,k})^2, \tag{3}$$

where $S_{2,k}$ is the set of the $n_{2,k}$ sample plots within the small area k, *Y(x)* stands for the observed hectare density of the target variable on the plot at point x (growing stock volume per ha or forest/non-forest decision). $Y_{2,k}$ is the sample mean of the hectare density of the plots in $S_{2,k}$.

A model prediction is calculated for each plot of the 500- $\times$500-m sampling grid within the small area. These model predictions (which can be arbitrary) are used for the following estimator:

$$\hat{Y}_{syn,k} = \frac{1}{n_{1,k}} \sum_{x \in s_1,k} \hat{Y}(x), \tag{4}$$

which is the *synthetic estimator* of the mean spatial density in the small area. Thereby, $s_{1,k}$ denotes the set of the $n_{1,k}$ sample plots in the first phase, and $\hat{Y}(x)$ is the predicted density of the target variable for the plot at point x.

The difference or small area estimator is defined as

$$\hat{Y}_{diff,k} = \hat{Y}_{syn,k} + \frac{1}{n_{2,k}} \sum_{x \in s_{2,k}} R(x), \tag{5}$$

where $R(x) = Y(x) - \hat{Y}(x)$ is the residual for the plot at point x (see Mandallaz 2008, formula 6.37). In large samples, one can treat so-called internal models (in which the model is fitted to the inventory data at hand) as external models (in which the regression coefficients are given). This estimator, in contrast to the synthetic estimator, is asymptotically design unbiased, and an asymptotically unbiased estimate of the design-based variance is then given by (see Mandallaz 2008, p. 81)

$$\hat{V}(\hat{Y}_{diff,k}) = \frac{1}{n_{1,k}} \hat{V}(Y(x)) + \left(1 - \frac{n_{2,k}}{n_{1,k}}\right) \frac{1}{n_{2,k}} \hat{V}(R(x)), \tag{6}$$

with

$$\hat{V}(R(x)) = \frac{1}{n_{2,k} - 1} \sum_{x \in s_{2,k}} (R(x) - R_{2,k})^2.$$

In this article, we refer to this estimator as difference estimator within the framework of a two-phase simple random sampling (according to Särndal et al. 1992). According to Mandallaz (2008), this is the standard regression estimator under two-phase sampling design with auxiliary information in the first phase (see also Baffetta et al. 2009, 2011). A special case is obtained with area-wide auxiliary information, for example, in the form of GIS-layers, which corresponds formally to n_1, $n_{1,\ k}$ going to infinity. The synthetic estimator is then

$$\hat{Y}_{syn,k} = \frac{1}{\lambda(G_k)} \int_{x \in G_k} \hat{Y}(x) dx, \tag{7}$$

where $\lambda(G_k)$ denotes the region of the small area. In this case,

$$\hat{V}(\hat{Y}_{diff,k}) = \frac{1}{n_{2,k}} \hat{V}(R(x)) \tag{8}$$

is the estimated design-based variance. In the present study, we compared difference estimators based on two types of prediction models: multiple linear regression models for the growing stock volume and logistic models for the attribute forest/non-forest. With linear regression models one cannot guarantee a priori that the predictions of growing stock volume, for example, are in a feasible range, i.e. positive and not unduly large. However, in the present study, these problems did not occur. The logistic model provides predictions $\hat{Y}(x)$, which are zero or one (according to whether the probability given by the logistic model is above 0.5 or not) as the $Y(x)$. Again, one can use the synthetic and small area estimators as for the $Y(x)$ and $\hat{Y}(x)$ pertaining to timber volume.

To assess the relative benefit of the difference estimator as compared to the direct estimation, we use the relative efficiency $RE = \hat{V}(\hat{Y}_{dir}) / \hat{V}(\hat{Y}_{diff})$ and the standard error $SE(\hat{Y}) = \sqrt{\hat{V}(\hat{Y})}$.

The statistical analysis was performed within the software environment R (R Development Core Team 2009). For the GIS routines, we used the rgdal (Keitt et al. 2010), sp (Pebesma & Bivand 2010) and raster (Hijmans & Etten 2010) libraries of R.

Results

Model Quality

The models predicting the proportion of forest with the canopy height resulted in proportions of correctly classified plots between 0.9 and 0.92 (see Table II). Adding the forest/non-forest decision from the aerial photograph interpretation as an explanatory variable resulted in 98% correctly classified plots no matter, which data were used (percentiles

Table II. Measures of goodness of fit for the different models.

GAMs Ancillary variables	Coefficients of determination Growing stock volume ADS	 Lidar	Proportion of plots correctly classified as forest/non-forest ADS	 Lidar
Terrestrial sampling				
Canopy height 95th (+ FNFd api)	0.61 (0.66)	0.61 (0.64)	0.90 (0.98)	0.91 (0.98)
Canopy height 90th (+ FNFd api)	0.62 (0.67)	0.62 (0.66)	0.92 (0.98)	0.91 (0.98)
Canopy height 75th (+ FNFd api)	0.63 (0.68)	0.66 (0.69)	0.91 (0.98)	0.91 (0.98)
Canopy height 50th (+ FNFd api)	0.65 (0.69)	0.68 (0.71)	0.92 (0.98)	0.91 (0.98)
Canopy height (+ FNFd api)	0.66 (0.69)	0.68 (0.71)	0.93 (0.98)	0.91 (0.98)
Forest samplings only				
Canopy height 95th	0.27	0.24		
Canopy height 90th	0.28	0.26		
Canopy height 75th	0.31	0.33		
Canopy height 50th	0.32	0.36		
Canopy height	0.30	0.37		

Note: Values in brackets indicate the coefficient of determination of models for which the forest/non-forest decision from the aerial photograph interpretation (FNFd api) was included. The mean tree heights were calculated for values above different percentiles, which are indicated by xth.
ADS, data from aerial stereo images; Lidar, data from the laser data.

used to calculate the mean canopy height together with aerial photography or Lidar data).

Models predicting the growing stock volume in the forest area showed a coefficient of determination ranging from 0.24 to 0.37 (see Table II). The Lidar data resulted in slightly better models compared to the aerial photography data when lower percentiles (50th or 0th) were used to build the mean tree heights.

The percentiles used to calculate the mean plot canopy height values had only a small impact on the goodness of fit. Independent of the data type (aerial photography versus Lidar), the simplest method of taking as auxiliary information the mean values of the canopy height within the quadrats around the sample plots generally performed best in predicting the growing stock volume. There is some evidence that the goodness of fit increases with the decreasing percentile used to derive the mean canopy height. Further explanatory variables related to the forest patchiness within the 25- $\times$25-m quadrats around the sample plots did not improve the model quality. Therefore, in the following, only results for small area estimations based on the simplest model (i.e. using the mean of all canopy height values within the 25- $\times$25-m quadrats) will be presented.

Direct Estimations

The direct estimation over the whole geographic area (Swiss Plateau and Jura mountains) yields a growing stock volume of 120 m^3/ha total area (SE = 3 m^3/ha) and a proportion of forest of 0.31 (SE = 0.01). This leads to a growing stock volume of 387 m^3/ha in the forested area. Within the small area, similar estimates are obtained when the 1.4- $\times$1.4-km grid or the 2- $\times$2-km grid are used (see Table III). With a further reduction of the sample size, the direct estimated growing stock volume increases to 182 m^3/ha total area (see the 4- $\times$4-km sample grid in Table III), with an estimated proportion of forest of 0.45. These estimates lead to a growing stock volume of around 404 m^3/ha in the forested area. The direct estimation per hectare forest area over the whole geographic area gives a result of 397 m^3/ha (SE = 6 m^3/ha). Within the small area, lower growing stock volumes are obtained with grids of higher densities. However, these differences are not significant (H_0 of the Mann-Whitney test for the differences of the mean growing stock volumes of the 1.4-km and the 4-km quadratic grid of the total area could not be rejected; $p = 0.06$. An analogous test for the mean growing stock volume within the forest area only resulted in a p value of 0.48). The direct estimation of the forest growing stock volume from the 2.8- $\times$2.8-km sampling grid gives a result of 393 m^3/ha, which is close to the direct estimate of the forest standing volume of the whole geographic area (see Table III).

Small Area Estimations

The usage of auxiliary information clearly led to a higher precision of estimates. Generally small area estimations based on Lidar data are slightly better than those based on aerial photography data.

Proportion of forest. The synthetic estimations of the proportion of forest did not depend on the sampling density (see Table IV). Compared to the aerial photography data, the synthetic estimations based on the Lidar data led to a slightly lower estimated proportion of forest (0.30 vs. 0.32). Models including the forest/non-forest decision of the aerial image interpretation resulted in an estimated proportion of forest of 0.36. Generally, the synthetic estimates are close to the direct estimates derived from the 1.4- $\times$ 1.4-km SNF grid. Including the forest/non-forest decision from the aerial image interpretation as an explanatory variable leads to higher synthetic estimates for the proportion of forest, no matter which data were used.

Table III. Direct estimations of the growing stock volume and the proportion of forest area with different sampling densities within the small area (whole Canton of Aargau).

	Sample grid over the area of the Canton Aargau			
	1.4 km	2 km	2.8 km	4 km
Growing stock volume per total area (m^3/ha)				
Mean	118	107	157	182
Standard error	8.53	10.71	21.12	34.47
Growing stock volume per forest area (m^3/ha)				
Mean	356	344	393	431
Standard error	16.76	20.47	37.74	60.65
Proportion of forest (%)				
Mean	0.34	0.33	0.42	0.45
Standard error	0.02	0.03	0.04	0.05

Table IV. Comparison of the synthetic estimator with the difference estimator of different models predicting the forest proportion.

			Difference estimations				
	Explanatory variables	Synthetic estimations	500 m × 500 m			Area-wide	
Small area	Proportion of forest	Mean	Mean	SE	RE	SE	RE
Aargau, 1.4 km	ADS	0.32	0.35	0.01	2.00	0.01	2.38
	ADS + FNFd api	0.36	0.35	0.01	6.25	0.00	25.00
	Lidar	0.30	0.35	0.01	2.13	0.01	2.56
	Lidar + FNFd api	0.36	0.36	0.01	7.14	0.00	50.00
Aargau, 2 km	ADS	0.32	0.34	0.02	2.17	0.02	2.38
	ADS + FNFd api	0.36	0.35	0.00	10.00	0.01	25.00
	Lidar	0.30	0.35	0.02	2.78	0.01	3.13
	Lidar + FNFd api	0.36	0.36	0.01	14.29	0.00	100.00
Aargau, 2.8 km	ADS	0.32	0.35	0.03	2.22	0.03	2.27
	ADS + FNFd api	0.36	0.34	0.01	10.00	0.01	14.29
	Lidar	0.30	0.34	0.02	2.33	0.02	2.44
	Lidar + FNFd api	0.36	0.35	0.01	12.50	0.01	20.00
Aargau, 4 km	ADS	0.32	0.35	0.04	1.89	0.04	1.92
	ADS + FNFd api	0.36	0.34	0.02	9.09	0.02	11.11
	Lidar	0.30	0.31	0.04	2.27	0.04	2.33
	Lidar + FNFd api	0.36	0.35	0.01	16.67	0.01	20.00

Note: All estimates are based on generalised linear models (GLMs).
ADS, auxiliary data from stereo-aerial images; Lidar, auxiliary data from airborne laser scanner data; FNFd api, forest/non-forest decision from the aerial photograph interpretation from the SNFI; SE, standard error; RE, relative efficiency (ratio of the estimated variance of the small area estimation to the observed variance).

For the denser sampling grids of 1.4 and 2 km, the difference estimators resulted in higher estimated proportion of forest compared to the direct estimators. In contrast, for the less dense sampling grids of 2.8 and 4 km, the difference estimators resulted in smaller proportions of forest compared to the direct estimators. Independent of the type of sampling grid, the synthetic estimates were generally close to the estimates from the difference estimator. Only in the case of the univariate Lidar-based models could a meaningful shift of the difference estimates be observed. A slightly higher precision was gained when the proportion of forest was estimated with the Lidar data compared to the aerial photography data (see Table IV: lower standard errors and as a consequence, higher relative efficiencies). Including the forest/non-forest decision in the models resulted in a clearly higher estimation precision.

Models based on the 1.4- × 1.4-km sample grid showed that using area-wide auxiliary information could potentially increase the relative efficiency by a factor of one fifth compared to the usage of a sample grid of 500 × 500 m. However, this potential gain in precision could not be observed in the models where the reduced data sets with smaller mesh size of 2.8 × 2.8 km or smaller were used.

In the case of the 500- × 500-m sampling density, adding the forest/non-forest decision from the aerial photograph interpretation distinctly increased the relative efficiency from values between 1.9 and 2.8 to values from around 6.2 to 16.7 (see Table IV). For area-wide auxiliary information, the relative efficiencies were within the range of 10 to 100 when the forest/non-forest decision from the aerial photograph interpretation was included.

Growing stock volume over the entire small area (forest and non-forested area). Estimated values from the synthetic estimators for the growing stock volume tend to be slightly though not significantly larger than the direct estimators (compare Table V with Table III).

By using the auxiliary data, we obtain relative efficiencies between 1.6 and 2.4 for the 1.4- × 1.4-km grid. With area-wide Lidar data (i.e. with n_1 going to infinity), the variance of the growing stock volume over the total area could be reduced to nearly one third of the observed variance (see the relative efficiency of 2.7 and 2.9 in Table V). With area-wide aerial photography data, the gain in precision was smaller but still a relative efficiency between 1.8 and 2.2 was reached. Including the forest/non-forest decision from the aerial images did not substantially improve the estimation precision of the growing stock volume.

Similar results were found when the estimates were calculated for the 4- × 4-km sample grid. However, when applying the same estimation procedures on the 2- × 2-km sample grid, the gain in precision was higher and the variance of the growing stock volume could be reduced to even one fourth of the observed variance when Lidar data were used on an area-wide basis and not merely on the plot level.

Table V. Comparison of the synthetic estimator with the difference estimator of different models predicting the growing stock.

Small area	Explanatory variables	Synthetic estimators	Difference estimators				
			500 m × 500 m			Area-wide	
		Mean	Mean	SE	RE	SE	RE
Aargau, 1.4 km		Standing volume (m^3/ha)					
	ADS	132	113	6.66	1.64	6.36	1.8
	ADS + FNFd api	136	118	6.18	1.91	5.78	2.18
	Lidar	123	120	5.74	2.21	5.24	2.66
	Lidar + FNFd api	129	122	5.54	2.37	4.99	2.93
		Standing volume in the forest (m^3/ha)					
	Forest decision based on api						
	ADS	397	341	14.78	1.28	14.52	1.33
	Lidar	360	345	14.56	1.32	14.26	1.38
	Forest decision based on the models						
	ADS	408	353	14.8	1.28	14.52	1.33
	Lidar	398	383	14.62	1.31	14.26	1.38
Aargau, 2 km		Standing volume (m^3/ha)					
	ADS	133	112	6.41	2.79	6.02	3.17
	ADS + FNFd api	138	114	5.98	3.21	5.52	3.76
	Lidar	121	114	5.86	3.36	5.38	3.98
	Lidar + FNFd api	125	117	5.71	3.53	5.21	4.25
		Standing volume in the forest (m^3/ha)					
	Forest decision based on api						
	ADS	422	348	16.22	1.59	15.91	1.65
	Lidar	360	329	16.17	1.6	15.89	1.66
	Forest decision based on the models						
	ADS	413	339	16.21	1.59	15.91	1.65
	Lidar	390	359	16.21	1.59	15.89	1.66
Aargau 2.8 km		Standing volume (m^3/ha)					
	ADS	134	131	15.17	1.92	14.95	2
	ADS + FNFd api	139	128	14.68	2.08	14.43	2.13
	Lidar	122	133	14.65	2.08	14.4	2.13
	Lidar + FNFd api	126	132	14.42	2.13	14.16	2.22
		Standing volume in the forest (m^3/ha)					
	Forest decision based on api						
	ADS	404	373	35.64	1.12	35.55	1.12
	Lidar	363	385	33.02	1.3	32.84	1.32
	Forest decision based on the models						
	ADS	418	388	35.64	1.12	35.55	1.12
	Lidar	392	414	33.05	1.3	32.84	1.32
Aargau 4 km		Standing volume (m^3/ha)					
	ADS	135	146	26.96	1.63	26.83	1.65
	ADS + FNFd api	139	141	26.11	1.74	25.96	1.76
	Lidar	121	135	26.12	1.74	25.96	1.76
	Lidar + FNFd api	126	137	25.83	1.78	25.67	1.8
		Standing volume in the forest (m^3/ha)					
	Forest decision based on api						
	ADS	405	401	61.47	0.97	61.48	0.97
	Lidar	363	406	55.76	1.18	55.66	1.19
	Forest decision based on the models						
	ADS	420	416	61.47	0.97	61.48	0.97
	Lidar	393	436	55.77	1.18	55.66	1.19

Note: The estimates of the growing stock volume are based on generalised additive models (GAMs). Note, however, that the estimation for the forest/non-forest decision used for estimating the growing stock volume within forest only is based on logistic regressions. The same notation is used for the abbreviations as in Table IV.

Growing stock volume (within the forest). The synthetic estimators of the denser sample grids (1.4 × 1.4 km and 2 × 2 km) resulted in higher values than the direct estimated growing stock volume per forest area of the terrestrial measurements. Accordingly, the difference estimators were corrected down to values closer to the observed forest growing stock volume. The synthetic estimates from the reduced sample grids (2.8 × 2.8 km and 4 × 4 km) were within the confidence intervals of the synthetic

estimates from the 1.4- × 1.4-km sample grid. The same was also valid for the difference estimates.

The gain in precision of the estimated forest growing stock volume neither depended on the data source (aerial photography vs. Lidar) nor on the type of forest decision (based on interpretation of the aerial images vs. the modelled forest-/non-forest decision) when calculated with the 1.4- × 1.4-km and 2- × 2-km sample grids. Compared to the aerial photography data, the usage of Lidar data resulted in higher precisions when the reduced sample grids of 2.8 × 2.8 km or 4 × 4 km were used to estimate the growing stock volume per forest area. Independent of the data source and the sample grid used, only marginal improvement in the estimation precision could be reached if area-wide auxiliary information were used to predict the growing stock volume per hectare forest.

Discussion

This study shows that using auxiliary information has great potential to improve the estimation of the growing stock volume as well as the proportion of forest within small areas. Generally, Lidar data proved to be slightly more suitable for the gain in precision for small area estimations than aerial photography data. The canopy height derived from the auxiliary data explained roughly 70% of the spatial variability of the growing stock volume per total area. Within forest areas only, Lidar heights explained up to 37% of the spatial variability of the growing stock volume whereas aerial photography data could explain at most 30% of the variance. Compared to Scandinavian studies where coefficients of determination of 0.8 or even higher were found between Lidar-derived canopy heights and the growing stock volume per hectare forest, the presented models are rather weak (Næsset 2002; Holmgren 2004, Magnussen et al. 2012). One probable reason for this is the higher species diversity and a higher complexity of the forest structure and topography in the region used for the present case study as compared to the monotone boreal forest type of the studies referred to above. A stratification of the sampling sites according to the slope and altitude would probably improve the models (Tonolli et al. 2011). The estimated growing stock volume depends not only on the canopy height but also on the tree species. The study by Næsset et al. (2004) showed for example that models for conifers deliver systematically deviant estimates for mixed forests, whereby the estimation error increased with an increasing proportion of deciduous tree species. Næsset (1997) also showed that the tree height and the stem volume do not correlate equally well for all species. It is also known that estimates for dense and inhomogeneous forests with a high proportion of broad-leaved tree species are less precise compared to estimates for sparse and homogeneous forest stands of conifers (Brandtberg et al. 2003). This might also explain why Hollaus et al. (2009) found higher correlations ($r^2 = 0.79$) compared to the findings presented in this study. Although the forest type in their study in the Montafon region (Austria) might be considered more similar to the temperate forest occurring in Switzerland compared to boreal forests, they report a considerably higher proportion of conifers compared to the mixed forests characterising the forest types of the Swiss Plateau and the Jura region. Furthermore, they also used a more complex regression model than was applied in this study. However, not only the species composition but also stand properties such as crown closure, height structure and ground vegetation have an effect on the correlation between the canopy height and the growing stock volume (Anttila 2002). The effect of the height structure and ground vegetation might be partly reflected when instead of using only the 5% topmost canopy height points the mean is used to predict the growing stock volume. That would explain why models based on mean values of the auxiliary data always resulted in higher coefficients of determination compared to values derived from percentiles. In addition, with increasing vegetation density, the estimation of tree height with remote sensing data becomes more difficult, especially in cases where neighbouring trees are taller than the trees within the plot. Such situations result in overestimations of the growing stock volume, as the above ground laser pulse height exceeds the measured height of the trees within the plot (Nord-Larsen & Riis-Nielsen 2010). On the other hand, it has to be noted that terrestrial tree height measurements are also not error free. The height of deciduous trees is especially difficult to measure during leaf-on conditions (Nord-Larsen & Riis-Nielsen 2010). Another potential source of uncertainty enters via location errors. Location errors occur due to various mechanisms including the incorrect location of sample plots using global positioning system. Often, geometric correction for remotely sensed data and mismatching image pixels and sample plots cause further location errors (Wang et al. 2011). In the case of the Swiss NFI, an imprecision of 10 m between the location of terrestrial samples and the remote sensing data is absolutely possible. However, with quite a large extraction window of 25 × 25 m, we intended to capture these potential errors of imprecise co-registration. Of course, the size of the extraction window used to calculate both the reference laser and image

metrics in turn influence model quality (Holopainen & Wang 1998). However, results from an earlier study showed that the window size of 25×25 m seems already optimal for modelling the forest growing stock volume (Steinmann et al. 2011).

Even though the quality of the models was moderate, the usage of remote sensing data clearly improved the estimation precision of both the proportion of forest and the growing stock volume.

The variance of the estimated growing stock volume per total area can be reduced to one fourth of the observed variance of the terrestrial measurements. This means that, when supported by remote sensing data, the same estimation precision can be gained with one fourth of the terrestrial samples as from the direct estimation using the total number of samples from the terrestrial SNFI data. It also means that with auxiliary data the estimation error (standard error) can be reduced to nearly one half of the direct estimated error. A study in northern Italy conducted in a forest composed mainly of Quercus and Carpinus reported an even higher reduction of the standard error when the estimation was Lidar assisted (Corona & Fattorini 2008). Using a model-based framework would probably lead to an even higher reduction of the variances (Ståhl et al. 2011). However, model-based estimators cannot be guaranteed to be unbiased. Therefore, because they are dependent on correct model specification, the models should be evaluated for quality of fit and systematic lack of fit (McRoberts 2006, 2011; McRoberts et al. 2007). As the presented models are rather weak, model-based estimates are not indicated in the presented case study.

The comparison of the estimation precision attained with the auxiliary data of the 500- $\times$ 500-m grid with the expected estimation precision generated with area-wide auxiliary data showed that the chosen density of a 500- $\times$ 500-m sampling grid is sufficient for most practical applications. With area-wide generated auxiliary data, the standard error was reduced to maximal 10%. Overall, the estimation precision for both the proportion of forest and the timber growing stock volume can clearly be increased with remote sensing data, (i.e. a variance reduction of up to two thirds was reached). Generally, the Lidar data led to slightly higher estimation precisions and higher reductions of standard errors compared to the data from aerial photography.

Conclusions

The study showed that the estimation precision for the proportion of forest and the growing stock volume can be significantly improved when supported by remotely sensed data. The precision of the small area estimations with Lidar data was slightly higher compared to the estimation based on data from aerial photography. However, data from aerial photography have the advantage that colour information could be used in the future for more specific models. Furthermore, new aerial photographs are regularly produced for the whole of Switzerland by Swisstopo. Therefore, canopy height information can be updated and thus changes in growing stock volume can easily be monitored. With a sample grid of 500×500 m for the auxiliary data, sufficiently precise estimates for most practical applications can be gained. With area-wide generated auxiliary data, a further variance reduction of maximal 10% could be achieved. However, such an effect would be too small to justify the exhaustive computation, which it would require.

Acknowledgements

We would like to thank Ann-Marie Jakob for greatly improving the linguistic aspect of the manuscript. In addition, we express our appreciation to the three anonymous reviewers whose valuable feedback helped us to substantially improve the scientific aspect of this article.

References

Anttila P. 2002. Nonparametric estimation of stand volume using spectral and spatial features of aerial photographs and old inventory data. Can J Forest Res. 32:1849–1857.

Baffetta F, Corona P, Fattorini L. 2011. Design-based diagnostics for *k*-NN estimators of forest resources. Can J Forest Res. 41:59–72.

Baffetta F, Fattorini L, Franceschi S, Corona P. 2009. Design-based approach to *k*-nearest neighbours technique for coupling field and remotely sensed data in forest surveys. Remote Sens Environ. 113:463–475.

Bohlin J, Wallerman J, Fransson JES. 2012. Forest variable estimation using photogrammetric matching of digital aerial images in combination with a high-resolution DEM. Scand J Forest Rese. 1–8, iFirst article. doi:10.1080/02827581.2012.686625.

Brändli, UB, editor. 2010. Schweizerisches Landesforstinventar: Ergebnisse der dritten Erhebung 2004–2006. Birmensdorf: Eidgenöss Forsch.anstalt Wald Schnee Landschaft; 312 p.

Brandtberg T, Warner TA, Landenberger RE, McGraw JB. 2003. Detection and analysis of individual leaf-off tree crowns in small footprint, high sampling density Lidar data from the eastern deciduous forest in North America. Remote Sens Environ. 85:290–303.

Breidenbach J, Astrup R. 2012. Small area estimation of forest attributes in the Norwegian National Forest Inventory. Eur J Forest Res. 131:1255–1267.

Corona P, Fattorini L. 2008. Area-based Lidar-assisted estimation of forest standing volume. Can J Forest Res. 38:2911–2916.

Franklin J. 1986. Thematic mapper analysis of coniferous forest structure and composition. Int J Remote Sens. 7:1287–1301.

Eid T, Gobakken T, Næsset E. 2004. Comparing stand inventories for large areas based on photo-interpretation and laser scanning by means of cost-plus-loss analyses. Scand J Forest Res. 19:512–532.

Ginzler C. 2005. Luftbildinterpretation LFI3: Interpretationsanleitung zum dritten Landesforstinventar. Birmensdorf: Eidgenössische Forschungsanstalt Wald Schnee und Landschaft; p. 16–19. German.

Gregoire TG. 1998. Design-based and model-based inference in survey sampling: appreciating the difference. Can J Forest Res. 28:1429–1447.

Gregoire TG, Ståhl G, Næsset E, Gobakken T, Nelson R, Holm S. 2011. Model-assisted estimation of biomass in a LiDAR sample survey in Hedmark County, Norway. Can J Forest Res. 41:83–95.

Hijmans RJ, van Etten J. 2010. Package 'raster': geographic analysis and modeling with raster data [Internet]. Version 1.5-16. [cited 2010 Dec 10]. Available from: http://raster.r-forge.r-project.org/

Hildebrandt G. 2010. The beginnings of aerial photogrammetry and interpretation in German forestry after 1945. Photogramm Fernerkun. 4:235–242.

Hollaus M, Dorigo W, Wagner W, Schadauer K, Höfle B, Maier B. 2009. Operational wide-area stem volume estimation based on airborne laser scanning and national forest inventory data. Int J Remote Sens. 30(19):5159–5175.

Holmgren J. 2004. Prediction of tree height, basal area and stem volume in forest stands using airborne laser scanning. Scand J Forest Res. 19(6):543–553.

Holmström H, Nilsson M, Ståhl G. 2001. Simultaneous estimations of forest parameters using aerial photograph interpreted data and the k nearest neighbour method. Scand J Forest Res. 16:67–78.

Holopainen M, Wang G. 1998. The calibration of digitized aerial photographs for forest stratification. Int J Remote Sens. 19(4):677–696.

Hudak AT, Crookston NL, Evans JS, Fallowski MJ, Smith AMS, Gessler PE, Morgan P. 2006. Regression modeling and mapping of coniferous forest basal area and tree density from discrete-return Lidar and multispectral satellite data. Can J Remote Sens. 32(2):126–138.

Katsch C, Stocker M 2000. Automatic determination of stand heights from aerial photography using digital photogrammetric systems. Allg Forst Jagdztg. 171:74–80.

Kaufmann E. 1999. Vorrat, Zuwachs, Nutzung. In: Brassel P, Lischke H, editors. Schweizerisches Landesforstinventar – Methoden und Modelle der Zweitaufnahme 1993–1995. Birmensdorf: Eidgenössische Forschungsanstalt Wald Schnee Landschaft; p. 162–196. German.

Keitt HT, Bivand R, Pebesma E, Rowlingson B. 2010. Package 'rgdal': bindings for the geospatial data abstration library [Internet]. Version: 0.6-28, [cited 2010 Dec 3]. Available from: http://www.gdal.org, http://sourceforge.net/projects/rgdal/

Kovats M. 1997. A large-scale aerial photographic technique for measuring tree heights on long-term forest installations. Photogramm Eng Remote Sens. 63(6):741–747.

Lanz A, Bierer D, Fringeli G, Mandallaz D. 2009. Neue Ansätze für die Waldinventur in der Schweiz. In: Thees, O, Lemm R, editors. Management zukunftsfähige Waldnutzung. Grundlagen, Methoden und Instrumente. Zürich: VDF; p. 361–377. German.

Latifi H, Nothdurft A, Koch B. 2010. Non-parametric prediction and mapping of standing timber volume and biomass in a temperate forest: application of multiple optical/LiDAR-derived predictors. Forestry. 83(4):395–407.

Magnussen S, Eggermont P, LaRiccia VN. 1999. Recovering tree heights from airborne laser scanner data. Forest Sci. 45(3):407–422.

Magnussen S, Næsset E, Gobakken T, Frazer G. 2012. A fine-scale model for area-based predictions of tree-size-related attributes derived from LiDAR canopy heights. Scand J Forest Res. 27:312–322.

Maltamo M, Packalén P, Suvanto A, Korhonen KT, Mehtätalo L, Hyvönen P. 2009. Combining ALS and NFI training data for forest management planning: a case study in Kuortane, Western Finland. Eur J Forest Res. 128:305–317.

Mandallaz D. 2008. Sampling techniques for forest inventories. Boca Raton: Chapman & Hall.

Mathys L, Ginzler C, Zimmermann NE, Brassel P, Wildi O. 2006. Sensitivity assessment on continuous landscape variables to classify a discrete forest area. Forest Ecol Manage. 229:111–119.

McCullagh P, Nelder JA. 1999. Generalized linear models. 2nd ed. Boca Raton: Chapman & Hall.

McRoberts RE. 2006. A model-based approach to estimating forest area. Remote Sens Environ. 103:56–66.

McRoberts RE. 2010. Probability- and model-based approaches to inference for proportion forest using satellite imagery as ancillary data. Remote Sens Environ. 114:1017–1025.

McRoberts RE. 2011. Satellite image-based maps: scientific inference or pretty pictures? Remote Sens Environ. 115:715–724.

McRoberts RE, Cohen WB, Næsset E, Stehman SV, Tomppo EO. 2010a. Using remotely sensed data to construct and assess forest attribute maps and related spatial products. Scand J Forest Res. 25:340–367.

McRoberts RE, Holden GR, Nelson MD, Liknes GC, Gormanson DD. 2006. Using satellite imagery as auxiliary data for increasing the precision of estimates for the Forest Inventory and Analysis program of the USDA Forest Service. Can J Forest Res. 36:2968–2980.

McRoberts RE, Tomppo EO, Finley AO, Heikkinen J. 2007. Estimating area means and variances of forest attributes using the k-Nearest Neighbors technique and satellite imagery. Remote Sens Environ. 111:466–480.

McRoberts RE, Tomppo EO, Næsset E. 2010b. Advances and emerging issues in national forest inventories. Scand J Forest Res. 25:368–381.

Næsset E. 1997. Estimating timber volume of forest stands using airborne laser scanner data. Remote Sens Environ. 61:246–253.

Næsset E. 2002. Predicting forest stand characteristics with airborne scanning laser using a practical two-stage-procedure and field data. Remote Sens Environ. 80:88–99.

Næsset E, Gobakken T, Holmgren J, Hyyppä H, Hyyppä J, Maltamo M, Nilsson M, Olsson H, Persson Å, Söderman U. 2004. Laser scanning of forest resources: the Nordic experience. Scand J Forest Res. 19:482–499.

Næsset E, Gobakken T, Solber S, Gregoire TG, Nelson R, Ståhl G., Weydahl D. 2011. Model-assisted regional forest biomass estimation using LiDAR and InSAR as auxiliary data: a case study from a boreal forest area. Remote Sens Environ 115:3599–3614.

Nord-Larsen T, Riis-Nielsen T. 2010. Developing an airborne laser scanning dominant height model from a countrywide scanning survey and national forest inventory data. Scand J Forest Res. 25:262–272.

Pebesma E, Bivand R. 2010. Package 'sp': classes and methods for spatial data [Internet]. Version 0.9-72. [cited 2010 Dec 10]. Available from: http://r-spatial.sourceforge.net/

R Development Core Team. 2009. R: a language and environment for statistical computing. Vienna, Austria: R Foundation for Statistical Computing.

Rao JNK. 2003. Small area estimation. Hoboken: Wiley.

Reese H, Nilsson M, Sandström P, Olsson H. 2002. Applications using estimates of forest parameters derived from satellite and forest inventory. Comp Electr Agric. 37:37–55.

Särndal CE, Swensson B, Wretman J. 1992. Model assisted survey sampling. Berlin: Springer.

Song C, Dickinson B, Su L, Zhang S, Yaussey D. 2010. Estimating average tree crown size using spatial information from Ikonos and QuickBird images: a cross-sensor and across-site comparisons. Remote Sens Enviro. 114:1099–1107.

Ståhl G, Holm S, Gregoire TG, Gobakken T, Næsset E, Nelson R. 2011. Model-based inference for biomass estimation in a LiDAR sample survey in Hedmark County, Norway. Can J Forest Res. 41:96–107.

Stehman SV. 2009. Model-assisted estimation as a unifying framework for area estimation of land cover and land-cover change. Remote Sens Environ. 113:2455–2462.

Steinmann K, Ginzler C, Lanz A. 2011. Combining data from the Swiss National Forest Inventory and from remote sensing for small-area estimations in forestry. Schweizerische Zeitschrift für Forstwesen. 162:290–299.

St-Onge B, Vega C, Fournier RA, Hu Y. 2008. Mapping canopy height using a combination of digital stereo-photo-grammetry and lidar. Int J Remote Sens. 29:3343–3364.

Tomppo E, Haakana M, Katila M, Peräsaari J. 2008. Multisource national forest inventory –methods and applications. Dordrecht: Springer.

Tonolli S, Dalponte N, Neteler M, Rodeghiero M, Vescovo L, Gianelle D. 2011. Fusion of airborne LiDAR and satellite multispectral data for the estimation of timber volume in the Southern Alps. Remote Sens Environ. 115:2486–2498.

Uuttera J, Haara A, Tokola T, Maltamo M. 1998. Determination of the spatial distribution of trees from digital aerial photographs. Forest Ecol Manage. 110:275–282.

Wang G, Zhang M, Gertner GZ, Oyana T, McRoberts RE, Ge H. 2011. Uncertainties of mapping aboveground forest carbon due to plot locations using national forest inventory plot and remotely sensed data. Scand J Forest Res. 26:360–373.

Waser LT, Ginzler C, Küchler M, Baltsavias E, Hurni L. 2011. Semi-automatic classification of tree species in different forest ecosystems by spectral and geometric variables derived from Airborne Digital Sensor (ADS40) and RC30 data. Remote Sens Environ. 115:76–85.

Waser LT, Klonus S, Ehlers M, Küchler M, Jung A. 2010. Potential of digital sensors for land cover and tree species classifications – a case study in the framework of the DGPF-Project. Photogram Fernerkun. 2:141–156.

Wolter PT, Townsend PA, Sturtevant BR, Kingdon CC. 2008. Remote sensing of the distribution and abundance of host species for spruce budworm in Northern Minnesota and Ontario. Remote Sens Environ. 112:3971–3982.

Wu Y, Strahler A. 1994. Remote estimation of crown size, stand density and biomass on the Oregon Transect. Ecol Appl. 4:299–312.